c)2001 American Institute of Aeronautics & Astronautics or Published with Permission of Author(s) and/or Author(s)' Sponsoring Organization.

7th AIAA/CEAS Aeroacoustics Conference
28-30 May 2001 Maastricht, Netherlands

A01-30882

AIAA 2001-2255

# Noise computation using Lighthill's equation with inclusion of mean flow - acoustics interactions*

Christophe Bogey[†] Christophe Bailly[‡] and Daniel Juvé[§]

Laboratoire de Mécanique des Fluides et d'Acoustique
Ecole Centrale de Lyon & UMR CNRS 5509
BP 163, 69131 Ecully cedex, France.

## Abstract

Lighthill's equation is used to compute the noise produced by subsonic flows. The objective is to show that, although this equation is based on a wave equation in a medium at rest, meanflow effects on sound propagation, included in Lighthill's source term, can be properly taken into account by numerical approches. The source terms are evaluated from the unsteady compressible flow motion equations, which provide also a reference sound field. By this way, all mean flow - sound waves interactions are included into the source terms. Two-dimensional cases are first considered with the radiation of a monopole in a sheared mean flow and with the sound generated by a mixing layer. They show that mean flow effects on propagation are correctly predicted with Lighthill's equation. The sound produced by pairings of axisymmetric vortices in a three-dimensional circular jet with a Mach number of 0.9 and a Reynolds number of 65000 is then investigated. Solving Lighthill's equation provides an acoustic radiation quite consistent with the sound field obtained directly from LES.

## 1. Introduction

The theory formulated by Lighthill in 1952[1] is considered as the starting point of modern aeroacoustics. It relies on an analogy between the full non linear flows and the linear theory of acoustics. The conservation equations are rewritten to form the following inhomogeneous wave equation

$$\left(\frac{\partial^2}{\partial t^2} - c_0^2\nabla^2\right)\rho = \frac{\partial^2 T_{ij}}{\partial x_i \partial x_j}(\mathbf{x}, t) \qquad (1)$$

where $\rho$ is the density, $c_0$ is the ambient sound speed and $T_{ij} = \rho u_i u_j + \left(p - c_o^2\rho\right)\delta_{ij} - \tau_{ij}$ is known as the Lighthill stress tensor, $u_i$, $p$, $\tau_{ij}$ being the velocity components, the pressure and the viscous stresses respectively. Lighthill's equation is exact since no approximation is made. Its classical interpretation consists in regarding the aerodynamic noise as solution of a wave equation in a fictitious medium at rest. The sound generation is attributed to the right-hand side of the equation, with a source term based on the Lighthill stress tensor. This tensor is reduced, in unheated flows at high Reynolds numbers, to the Reynolds stresses $\rho u_i u_j$. Practically, by using Green function of the wave equation, the solution of equation (1) is written as an integral on a region encompassing all sound sources. The integral solution of Lighthill's equation has first allowed to establish, by a dimensional analysis, the scaling law of the acoustic power for a subsonic jet as the eight power of the jet velocity. It can also be used to determine directly the noise, but this requires an accurate estimation of the sound sources, through $T_{ij}$.

The method for predicting noise using Lighthill's equation is usually referred to as an hybrid method since noise generation and propagation are treated separately. The first step consists in using data provided by numerical simulations to form the sound sources. The second step then consists in solving the wave equation forced by these source terms to determine the sound radiation. The main advantage of this approach is that most of the conventional flow simulations can be used in the first step. By this way, the mean turbulent parameters of flows computed by solving the Reynolds Averaged Navier-Stokes equations (RANS) with a $k-\epsilon$ turbulent closure can be introduced in a statistical source model[2] to obtain the acoustic intensity.[3] It is naturally more convenient to use the unsteady flow parameters to evaluate directly $T_{ij}$. It has been done successfully to

*Copyright @ 2001 by the Authors. Published by the American Institute of Aeronautics and Astronautics, Inc., with permission.

†Research scientist CNRS, Member AIAA
‡Assistant Professor, Member AIAA
§Professor, Member AIAA

c)2001 American Institute of Aeronautics & Astronautics or Published with Permission of Author(s) and/or Author(s)' Sponsoring Organization.

compute the acoustic field generated by turbulent flows, using the data obtained by solving the unsteady RANS,[4] by Large Eddy Simulation (LES)[5–7] or by Direct Numerical Simulation (DNS).[8,9]

However, one important difficulty of Lighthill's equation is that there is not a complete separation between aerodynamics and acoustics. The wave operator being a classical wave equation in a medium at rest, all interactions between flow and acoustic waves are included into the right-hand side of the equation, namely in the source term. Further developments have so been carried out to put some mean flow effects on sound propagation into the wave operator, by Phillips[10] and Lilley[11] particularly. Lilley has combined the flow motion equations to obtain a wave operator based on a third-order differential equation accounting for effects of a unidirectional sheared mean flow on sound propagation.[12] The use of the Linearized Euler Equations (LEE) as wave operator has also been proposed because all mean flow effects on propagation can be included into the LEE for general flows and geometries.[13]

To compute noise using Lighthill's equation when interactions between flow and acoustic waves are significant, basically for high Mach number flows, it is necessary to evaluate the source term accuratly since it contains these interactions. This implies that the simulation providing source terms must be compressible. The only exception is found for a uniform mean flow where a convected Green function can be used. In the general case, equation (1) must be integrated on the smallest region including both sound sources and flow - acoustics interactions. The two contributions of the source term are moreover clearly identified in the Lighthill tensor $T_{ij}$. Sound generation by turbulence is associated to the terms quadratic in velocity fluctuations, whereas mean flow effects on wave propagation, namely refraction and convection, are associated to the terms linear in fluctuations. These two parts of Lighthill's tensor are classically called the self-noise and the shear-noise[14] respectively.

The motivation of this study is to investigate the computation of the sound by solving Lighthill's equation for subsonic flows, and to show that interactions between mean flow and acoustic waves are properly taken into account provided that they are included into the right-hand side of the equation. The source terms are formed from data obtained by solving the unsteady compressible flow equations. The acoustic field is also directly found by this way and it constitutes a reference solution to compare to the result given by Lighthill's equation. Three cases are considered. The first one is purely acoustic and concerns the propagation in a sheared mean flow of the sound generated by a monopolar source. The second one involves a two-dimensional mixing layer excited to control the first vortex pairings,[6] which generate an acoustic radiation at a fixed frequency. The third one is a circular three-dimensional jet excited to force the development of axisymmetric vortices, whose pairings produce a sound field classically associated to axisymmetric sources. In the three cases, equation (1) is integrated on a region containing all sound sources, extending in the direction of the observer as far as there are mean flow effects on sound propagation. Results are compared to solutions provided directly by the flow motion equations or given by the hybrid method using LEE, in order to study the contribution of the part of the Lighthill tensor associated to propagation.

This paper is organized as follows. Effects of a sheared mean flow on the radiation of a monopolar source are investigated in section 2. The sound field generated by a mixing layer is studied in section 3. Next, in section 4, the noise generated by pairings of axisymmetric vortices in a subsonic jet is calculated. Finally, concluding remarks are given in section 5. The frequency domain solution of Lighthill's equation used in this study for two-dimensional geometries is presented in Appendix A.

## 2. Propagation of the sound radiated by a monopolar source in a sheared mean flow

### 2.1 Definition

We first consider an acoustic monopole placed in a sheared mean flow, as illustrated in Figure 1.

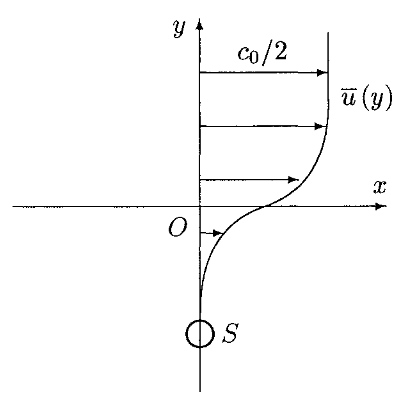


Figure 1: Sketch of the monopolar source $S$ located in the sheared mean flow $\overline{u}(y)$.

The domain extends from -50 up to 50 meters in the two coordinates directions. The mean flow is a

c)2001 American Institute of Aeronautics & Astronautics or Published with Permission of Author(s) and/or Author(s)' Sponsoring Organization.

shear layer between a medium at rest and a uniform flow with a velocity equal to half the mean sound speed $c_0$. Its expression is given by the hyperbolic-tangent profile

$$\bar{u}(y) = \frac{c_0}{4}\left[1 + \tanh\left(\frac{2y}{\delta_\omega}\right)\right]$$

where the vorticity thickness is taken as $\delta_\omega = 20$m.

A Gaussian monopolar source is introduced at the point $(0, -30\text{m})$ where the mean flow is negligible. To define a purely acoustic problem, two source terms are added into the equations governing pressure and density respectively, by the following way

$$\begin{cases} \dfrac{\partial p}{\partial t} = \ldots + \epsilon \sin(\omega t) \exp\left[-\ln(2)\left(x^2 + y^2\right)/b^2\right] \\ \dfrac{\partial \rho}{\partial t} = \ldots + \dfrac{\epsilon}{c_0^2} \sin(\omega t) \exp\left[-\ln(2)\left(x^2 + y^2\right)/b^2\right] \end{cases}$$

where the pulsation $\omega$ is fixed so that the wavelength is $\lambda = 18$m, the amplitude is $\epsilon = 1$Pa and the Gaussian half-width is $b = 3$m. The amplitude is weak enough to have a linear sound propagation. The vorticity thickness of the shear layer and the acoustic wavelength are also very close. So, both convection and refraction effects on propagation will occur.

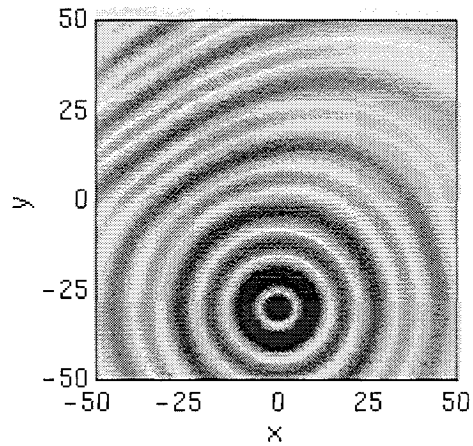


Figure 2: Monopolar source in a sheared mean flow. Pressure field obtained by solving Euler's equations. The color scale is defined for levels from -3×10$^{-3}$ to 3×10$^{-3}$ Pa.

### 2.2 Reference solution provided by Euler's equations

The propagation of sound waves can be computed using the full Euler equations. In this purely acoustic case, these equations are solved to provide both a reference solution and the source term of Lighthill's equation. A uniform mesh is used with constant grid size $\Delta x = \Delta y = 1$m and the time step is $\Delta t = c_0 \times 2/3$ s. The pressure field given by Euler's equations is presented in Figure 2. Effects of the mean flow on sound propagation are clearly visible. Circular wave fronts are significantly deformed in the upper part of the domain.

To estimate more precisely the modification of sound propagation induced by the sheared mean flow, the simulation is also performed without the presence of mean flow. The pressure field obtained by this way is subtracted to the previous field to obtain the pressure field shown in Figure 3. This one is only attributed to the mean flow effects on sound propagation. The interations between flow and acoustic waves are not so weak since its amplitude is of the order of the amplitude of the incident radiation.

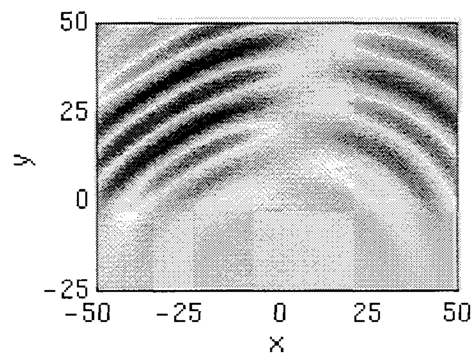


Figure 3: Monopolar source in a sheared mean flow. Difference between the two pressure fields obtained by solving Euler's equations with and without the mean flow respectively. Only the domain $y \geq -25$m is shown. The color scale is the same as in Figure 2.

### 2.3 Resolution of Lighthill's equation

Lighthill's equation is now solved using the frequency-domain integral solution (6) given in Ap-

c)2001 American Institute of Aeronautics & Astronautics or Published with Permission of Author(s) and/or Author(s)' Sponsoring Organization.

pendix A. The Lighthill tensor $T_{ij} = \rho u_i u_j$ is evaluated from the Euler simulation carried out with the sheared mean flow. It is stored every time steps during an acoustic period, with 27 recordings. The source region is the whole domain so that all mean flow - sound wave interactions are integrated.

The pressure field obtained by this way is presented in Figure 4. It corresponds very well to the field of Figure 3. The agreement between the two fields is shown more quantitatively in Figure 5 with the pressure profiles at $y = 30$ m. In this case where fluctuations are only acoustic and small enough so that the propagation is linear, the only contribution of Lighthill's tensor is related to mean flow - acoustics interactions. They are well accounted for in Lighthill's equation to provide all effects of the mean flow on propagation of the incident sound waves. The same result has been recently shown in a similar configuration for the volume integral of the Ffowcs Williams & Hawkings equation.[15]

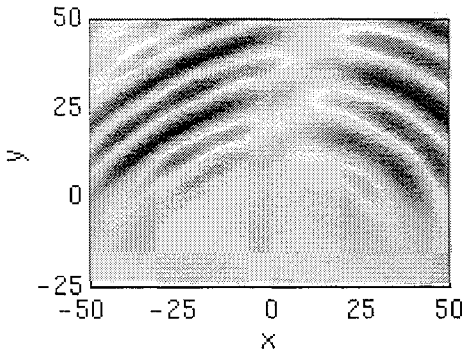


Figure 4: Monopolar source in a sheared mean flow. Pressure field obtained by solving Lighthill's equation. Only the domain $y \geq -25$m is shown. The color scale is the same as in Figure 2.

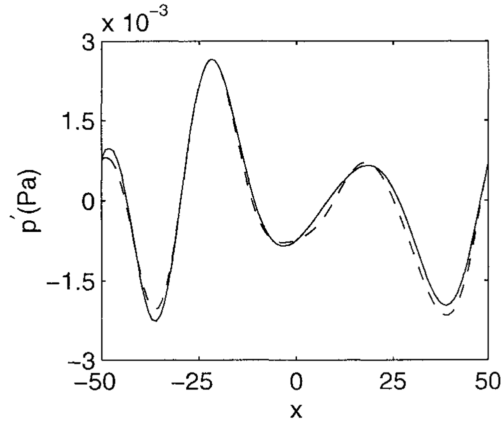


Figure 5: Monopolar source in a sheared mean flow. Pressure profiles at $y = 30$m obtained by solving: ——— Euler's equations (difference between the pressure fields obtained with and without mean flow), − − − Lighthill's equation.

## 3. Sound field generated by a mixing layer

### 3.1 Definition and reference solution

This second application involves a subsonic mixing layer between two uniform flows at $U_1 = 40$ and $U_2 = 160$ m.s$^{-1}$, with a Reynolds number based on the initial vorticity thickness $\delta_\omega(0)$ equal to $Re_\omega = 12800$. This flow has been simulated by Large Eddy Simulation (LES) in a previous study. All the details of the simulation can be found in Bogey *et al.*[6] The mixing layer is forced at its fundamental frequency $f_0$[16] and its first sub-harmonic frequency $f_0/2$ to fix the location of vortex pairings around $x \simeq 70\delta_\omega(0)$. By this way, the sound field generated by the first vortex pairings is investigated. It shows an acoustic wavelength $\lambda_p = 51.5\delta_\omega(0)$, corresponding to the pairing frequency $f_p = f_0/2$ and to the pairing period $T_p = 330$ iterations of the LES.

A reference acoustic field is provided directly by LES on a domain extending from 0 up to 200 $\delta_\omega(0)$ in the axial direction and from -300 $\delta_\omega(0)$ up to 300 $\delta_\omega(0)$ in the transerve direction. It has been previously compared to results given by applying a three-dimensional solution of Lighthill's equation.[6] It has also allowed to validate the expression of source terms used in the hybrid method based on LEE.[13]

In this configuration, mean flow - acoustic interactions are important, particularly owing to the two uniform flows. The source term used in Lighthill's equation must provide both sound generation and mean flow effects on propagation.

### 3.2 Resolution of Lighthill's equation

Lighthill's equation is solved in the frequency-domain as shown in Appendix A, using source terms issued from LES data. The source terms are recorded every 30 time steps during 2640 iterations, i.e. during 8 pairing periods. They are known on the whole computational domain to account for all mean flow - sound wave interactions. Furthermore, to study the two contributions in Lighthill's tensor, two source terms are considered. The first one, $T^f_{ij} = \rho u'_i u'_j$ where $u'_i$ are the velocity fluctuations, corresponds to the self-noise and provides only the sound generation by turbulence. The second one, $T^t_{ij} = \rho u_i u_j$, corresponds to the complete Lighthill's tensor.

c)2001 American Institute of Aeronautics & Astronautics or Published with Permission of Author(s) and/or Author(s)' Sponsoring Organization.

### 3.3 Pressure fields

The pressure fields obtained by solving Lighthill's equation on the whole domain using source terms $T_{ij}^f$ and $T_{ij}^t$ are presented in Figures 6(a) and 6(b) respectively. They are strongly different, both in terms of wave front pattern and directivity.

Waves fronts obtained using $T_{ij}^f$ are quite circular, centered on the region of pairings. Directivity of the sound radiation is well marked into the downstream direction, especially for the low-velocity flow in the lower part. The radiation pattern calculated using $T_{ij}^t$ displays waves fronts significantly ovalized by the two uniforms flows. The directivity is also modified and is now pronounced for rather large angles from the downstream direction, around $\theta = 60°$.

Integrating Lighthill's equation on the whole observation region using the complete Lighthill tensor allows to account for mean flow effects on sound propagation, even in this flow configuration with two surrounding uniform flows.

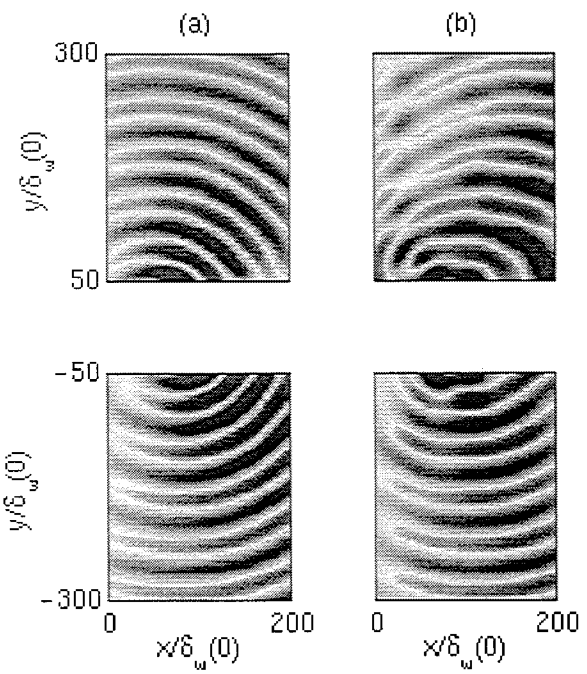


Figure 6: Sound generated by a mixing layer. Pressure fields computed with Lighthill's equation by using source term: (a) $T_{ij}^f$ and (b) $T_{ij}^t$. The color scale is defined for levels from -8 to 8 Pa.

### 3.3 Dilatation fields and comparison

To compare the sound field given by Lighthill's equation with results provided by LES and by the hybrid method based on LEE, the dilatation $\Theta = \nabla.\mathbf{u}$ is used. Dilatation is connected to the acoustic pressure by the relation

$$\Theta = -\frac{1}{\rho_0 c_0^2}\frac{\partial p'}{\partial t} \qquad (2)$$

in a medium at rest, $\rho_0$ and $c_0$ being the ambient density and sound speed, and by

$$\Theta = -\frac{1}{\rho_0 c_0^2}\left(\frac{\partial p'}{\partial t} + U_i\frac{\partial p'}{\partial x}\right) \qquad (3)$$

in a uniform flow of velocity $U_i$.

The dilatation fields provided by Lighthill's equation with source terms $T_{ij}^f$ and $T_{ij}^t$ are thus calculated using relations (2) and (3) respectively. They are shown in Figures 7(a) and 7(c) and compared with results given by other prediction methods.

The dilatation field obtained with $T_{ij}^f$ is beside the dilatation field of Figure 7(b) given by LEE solved without the presence of mean flow. There is a good agreement between the two fields. The directivities are the same, both are well marked into the downstream direction. Wave fronts are in phase and have similar amplitude. This is shown more quantitatively in Figure 9 with the dilatation profiles at $x = 130\delta_\omega(0)$. The two methods applied, Lighthill's equation forced with $T_{ij}^f$ and LEE solved without mean flow, combine a wave operator in a medium at rest with source terms corresponding only to the sound generation, the so-called self-noise, that explains the accordance between the two results.

The dilatation field obtained by solving Lighthill's equation with $T_{ij}^t$ is compared to the dilatation field of Figure 7(d) directly provided by LES. The two fields agree very well. The directivities are affected in the same way by the mean flow with a preferred radiation for angles from the downstream direction around $\theta = 80°$ in the low-velocity flow, and $\theta = 60°$ in the high-velocity flow. The modifications of the wave front pattern are also the same. It is confirmed by Figure 8 plotting the dilatation profiles at $x = 130\delta_\omega(0)$, around $60\delta_\omega(0)$ downstream the sound sources, in a region where the wave fronts are significantly deformed by the mean flow. The two profiles superimpose, demonstrating the very good agreement in phase and in amplitude. Therefore, by solving Lighthill's equation with the complete Lighthill tensor, all interactions between flow and sound waves are properly taken into account.

This application shows that it is possible, using Lighthill's equation, to compute the sound generated by a turbulent flow accounting for mean flow effects on sound propagation, if these interactions are correctly included in the Lighthill tensor.

c)2001 American Institute of Aeronautics & Astronautics or Published with Permission of Author(s) and/or Author(s)' Sponsoring Organization.

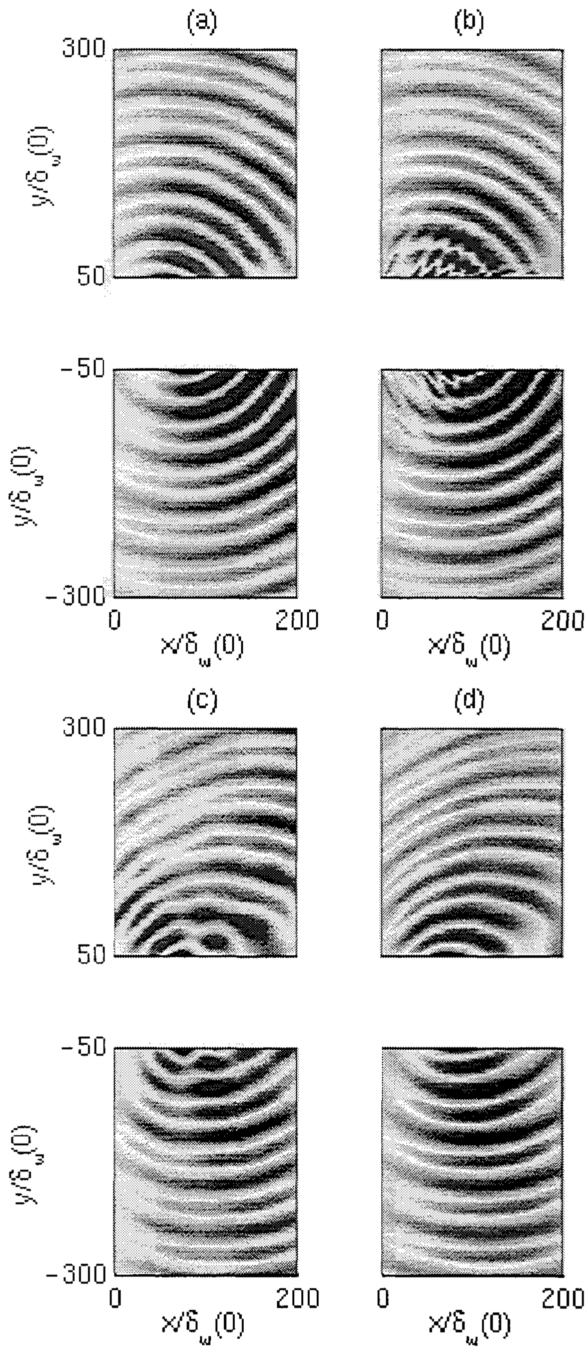


Figure 7: Sound generated by a mixing layer. Dilatation fields obtained at the same time: by solving Lighthill's equation using (a) $T^f_{ij}$ and (c) $T^t_{ij}$, (b) by LEE without mean flow, (d) by LES. The color scale is defined for levels from -1.5 to 1.5 $s^{-1}$.

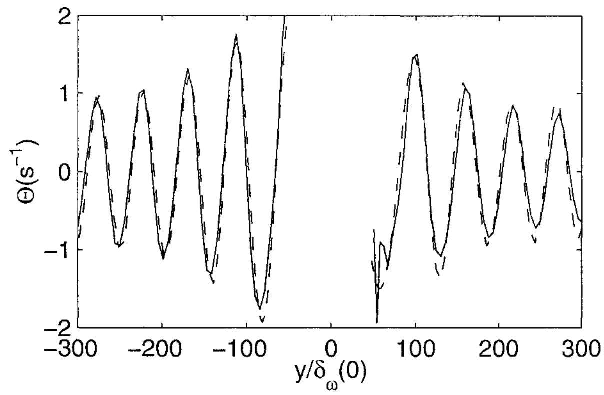


Figure 8: Sound generated by a mixing layer. Dilatation profiles at $x = 130\delta_\omega(0)$ obtained by solving: ——— LEE without mean flow, – – – Lighthill's equation using $T^f_{ij}$.

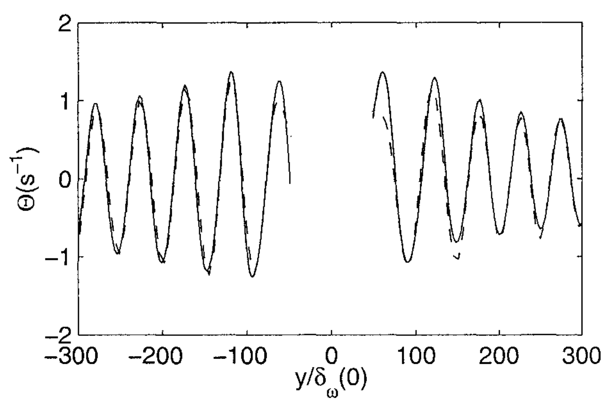


Figure 9: Sound generated by a mixing layer. Dilatation profiles at $x = 130\delta_\omega(0)$ obtained: ——— by LES, – – – , by solving Lighthill's equation using $T^t_{ij}$.

c)2001 American Institute of Aeronautics & Astronautics or Published with Permission of Author(s) and/or Author(s)' Sponsoring Organization.

## 4. Sound field generated by a circular jet excited axisymmetrically

### 4.1 Definition and flow simulation

The third application of this paper involves a three-dimensional computation. A circular jet with a Mach number of 0.9 and a Reynolds number of $6.5 \times 10^4$ is simulated by Large Eddy Simulation. The ratio $r_0/\delta_\theta$ is 20, where $r_0$ is the initial jet radius and $\delta_\theta$ is the momentum thickness of the shear layer. In a previous study,[17] the jet was forced into the inflow randomly both in space and time, to investigate its natural turbulent development and the corresponding generated acoustic radiation. In this study, it is excited axisymmetrically, at the fundamental frequency $f_0$ and the first sub-harmonic frequency $f_0/2$ of the initial hyperbolic-tangent velocity profile. By this way, vortex rings are created in the shear layer. They merge at a fixed location at the frequency $f_p = f_0/2$ to form a larger vortex ring.

LES is carried out using the ALESIA code,[17] built up with numerical methods specific to aeroacoustics in order to compute directly the acoustic field. In the code, the Smagorinsky subgrid scale model is used. All the details of the simulation can be found in Bogey.[18] The cartesian mesh grid consists of $127 \times 177 \times 127$ points, with 28 points in the jet radius. It extends up to $x = 22r_0$ in the axial direction, and up to $y = 22r_0$ in the $y$ direction to study the acoustic radiation in the upper $x - y$ section. Meshes are moreover significantly stretched from $x = 8r_0$ in the axial direction, in order to damp the aerodynamic perturbations downstream. Finally, the simulation runs for $1.2\times10^4$ iterations. The pairing period corresponds to $T_p = 300$ iterations.

Four snapshots of the vorticity $\omega_z$ regularly spaced over a period $T_p$ are shown in Figure 10. Pairings of vortex rings occur around $x = 4.5r_0$ every $T_p$. There are no other pairing downstream and the created vortex ring is dissipated in the sponge region. Collision of vortex rings constitutes a classical sound source.[19] The sound generated in the jet by this mechanism is now investigated.

### 4.2 Sound field computed by LES

The dilatation field $\Theta = \nabla.\mathbf{u}$ directly provided by LES is presented in Figure 11. Dilatation is here proportional to time derivative of the acoustic pressure as $\Theta = -(\partial p'/\partial t)/(\rho_0 c_0^2)$. Wave fronts are visibly coming from the pairing region around $x = 4.5r_0$. The predominant wavelength corresponds to the pairing frequency with $\lambda_p = 6.6r_0$. The noise

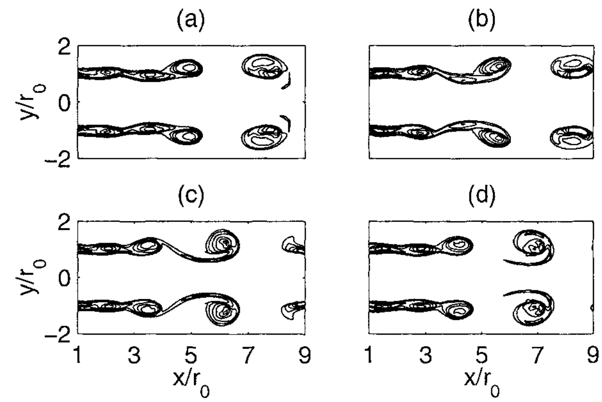


Figure 10: Circular jet excited axisymmetrically. Snapshots of the vorticity field $\omega_z$ in the $x-y$ plane at $z = 0$, at four times separated of $T_p/4$. Vorticity contours are $[2,3,4,5,6,7]\times10^5$ s$^{-1}$.

generated by the excitation into the inflow is non negligible but it is small compared to the sound field produced by pairings.

The sound field has an angle of extinction around $\theta \simeq 80°$ from the jet axis. It is given more precisely in Figure 12 with the directivity of the acoustic radiation. This particular directivity is inherent in excited jets and it is not found for natural turbulent jets. To illustrate this, the sound pressure levels calculated for the jet excited with a random noise are also shown in Figure 12. For comparison, levels are normalized at a distance of $60r_0$ from the region of sound generation. Levels in the two cases are of the same order, but the directivities are basically different.

The directivity found in this study is classically attributed to the radiation of axisymmetric quadrupolar sources. It has been investigated theoretically for a compact source using Möhring's analogy[20,21] and Lighthill's analogy.[8,22] The directivity of an axisymmetric quadrupole, compact in the radial direction, is given by the function $3\cos^2\theta - 1$. Two angles of extinction of the sound field are thus predicted for $\theta = 55°$ and $\theta = 125°$. This directivity pattern has been found experimentally by Bridges & Hussain,[21] by exciting a Mach 0.08 jet with discrete frequencies, with an angle of extinction for $\theta = 70°$. It has also been found recently in axisymmetric simulations, by Bastin[22] for a Mach 0.58 jet and by Mitchell *et al.*[8] for Mach 0.4 and Mach 0.8 jets. In these numerical studies, angles of extinction are in the range $\theta = 60° - 70°$.

In the present study, the angle of extinction of the sound field is $\theta \simeq 80°$. The discrepancy with

c)2001 American Institute of Aeronautics & Astronautics or Published with Permission of Author(s) and/or Author(s)' Sponsoring Organization.

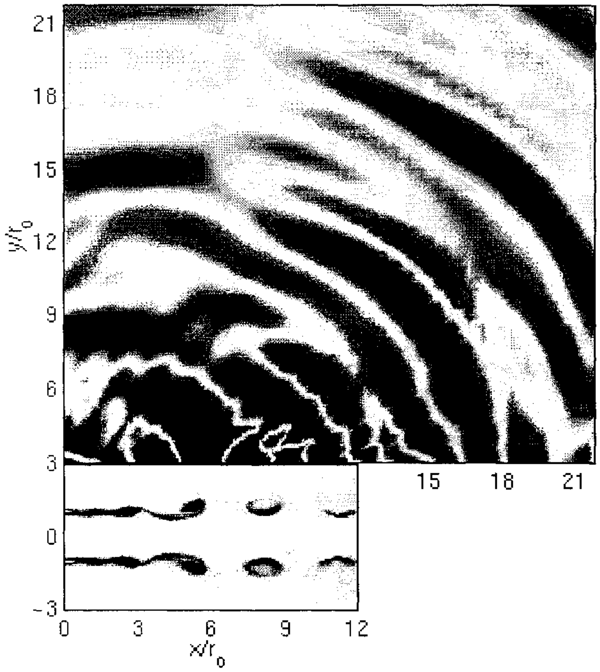


Figure 11: Circular jet excited axisymmetrically. Snapshot of the dilatation field in the acoustic region, and of the vorticity field $\omega_z$ in the flow region, in the $x-y$ plane at $z = 0$. The dilatation color scale is defined for levels from -90 to 90 $s^{-1}$, the vorticity scale for levels from $-6\times10^5$ to $6\times10^5$ $s^{-1}$.

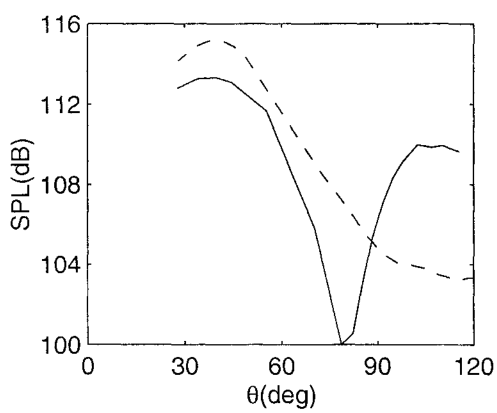


Figure 12: Circular jet excited axisymmetrically. ——— sound pressure levels at $60r_0$ from the pairing region as function of angle $\theta$ measured from the jet axis, $- - -$ levels generated by the jet randomly excited, at $60r_0$ from the end of the potential core.

the theoretical angle and with experimental or others numerical results can be explained by our jet parameters. The sound source is first not fully compact in the radial direction since $\lambda_p = 6.6r_0$. The jet velocity is also very high with a Mach number of 0.9. Thus, one can expect that the flow affects strongly the propagation of sound waves. Finally, the parasitic radiation associated to the excitation can be suspected, because its effects are larger where the amplitudes of sound waves are small, near the angle of extinction.

### 4.3 Resolution of Lighthill's equation

A time-domain solution of Lighthill's equation, built up from a three-dimensional Green function, is solved to compute the noise radiated by the jet. This integral formulation involves time derivatives, and it is more accurate than the integral formulation with space derivatives.[6] Its far-field expression is written as

$$p'(\mathbf{x}, t) = \frac{1}{4\pi c_0^2} \int_{V_y} \frac{r_i r_j}{r^3} \frac{\partial^2 T_{ij}}{\partial t^2} \left(\mathbf{y}, t - \frac{r}{c_0}\right) d\mathbf{y} \quad (4)$$

The tensors $T_{ij}^f = \rho u_i' u_j'$ and $T_{ij}^t = \rho u_i u_j$ are recorded every 10 aerodynamic time steps, during 2400 iterations corresponding to 8 pairing periods. Every points in the axial direction, and every second points in the two other directions are taken from the LES mesh grid. The source volume $V_y$ is such that $r_0 \leq x \leq 20.5r_0$ and $-3.4r_0 \leq y, z \leq 3.4r_0$. It is large enough to contain the whole region where there are mean flow - sound waves interations. These interactions are indeed negligible outside the jet, where the mean axial velocity is very small as shown in Figure 13.

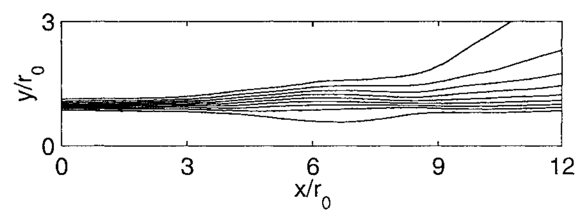


Figure 13: Circular jet excited axisymmetrically. Mean axial velocity at $z = 0$: 9 contours defined from $0.1\times U_j$ to $0.9\times U_j$ with a constant increment of $0.1\times U_j$, where $U_j$ is the jet exit velocity.

The two kinds of source terms $(1/c_0^2)\ \partial^2 T_{ij}^f/\partial t^2$ and $(1/c_0^2)\ \partial^2 T_{ij}^t/\partial t^2$ are displayed in Figures 14 and 15 respectively. There is no significant truncation of

c)2001 American Institute of Aeronautics & Astronautics or Published with Permission of Author(s) and/or Author(s)' Sponsoring Organization.

the source terms at the boundaries of the source region. Moreover, the two radial source terms based on $T_{22}$ are very similar, whereas the axial and cross source terms based on $T_{11}$ and $T_{12}$ are quite different, the larger differences being found for the axial source term. The mean flow effects on wave propagation, essentially induced by the axial velocity, are therefore very small perpendicularly to the jet axis, but increase significantly closer to the axial direction.

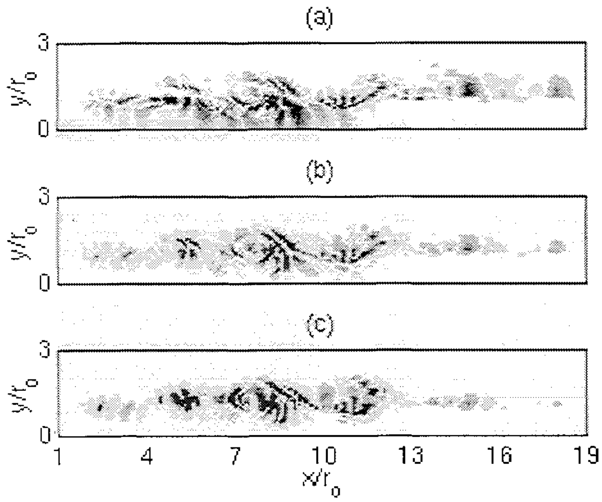


Figure 14: Circular jet excited axisymmetrically. Source terms used in Lighthill's equation, shown at $z = 0$ : (a) $(1/c_0^2)\ \partial^2 T_{11}^f/\partial t^2$, (b) $(1/c_0^2)\ \partial^2 T_{12}^f/\partial t^2$, (c) $(1/c_0^2)\ \partial^2 T_{22}^f/\partial t^2$ . The color scale is defined for levels from $-10^{10}$ to $10^{10}$ kg.m$^{-3}$.s$^{-2}$.

To compare the sound field predicted by Lighthill's equation with the LES result, the time evolution of pressure is determined during a period $T_p$ at points located in the acoustic far-field at $60r_0$ from the pairing region, for angles in the range $30^o - 120^o$. The sound pressure levels obtained by this way are shown in Figure 16. The two directivities found using $T_{ij}^f$ and $T_{ij}^t$ are similar for $\theta > 80^o$ but are quite different for smaller angles. The acoustic radiation computed using $T_{ij}^f$, the self-noise alone, is well pronounced in the downstream direction, whereas the sound field computed using $T_{ij}^t$ is marked for an angle around $\theta \simeq 40^o$. This angle is also found in the LES sound field. It can be attributed to refraction effets of sound waves by the flow. Solving Lighthill's equation using the complete Lighthill tensor has thus allowed to provide the good directivity, with both the angles of maximum and minimum radiation. Levels given by Lighthill's equation are also consistent with the LES solution near the angle of

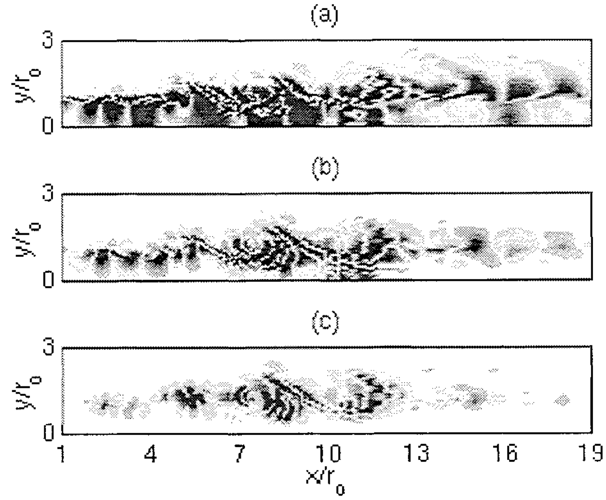


Figure 15: Circular jet excited axisymmetrically. Source terms used in Lighthill's equation, shown at $z = 0$ : (a) $(1/c_0^2)\ \partial^2 T_{11}^t/\partial t^2$, (b) $(1/c_0^2)\ \partial^2 T_{12}^t/\partial t^2$, (c) $(1/c_0^2)\ \partial^2 T_{22}^t/\partial t^2$. The color scale is the same as in Figure 15.

extinction. The agreement is however not so good in the downstream direction with a significant difference between the direct calculation and Lighthill's prediction. At this time, we have no explanation for this disagreement.

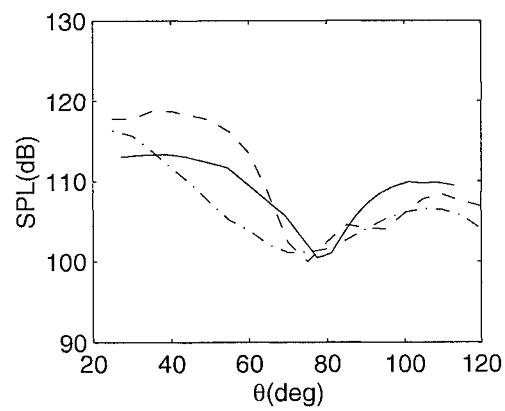


Figure 16: Circular jet excited axisymmetrically. ——— sound pressure levels at $60r_0$ from the pairing region given by LES, $- \cdot - \cdot$ levels obtained with Lighthill's equation using $T_{ij}^f$, $- - -$ levels obtained with Lighthill's equation using $T_{ij}^t$.

## 5. Conclusion

This study shows that Lighthill's equation is able to provide aerodynamic noise, accounting for mean

c)2001 American Institute of Aeronautics & Astronautics or Published with Permission of Author(s) and/or Author(s)' Sponsoring Organization.

flow effects on sound propagation. This equation being based on a wave equation in a medium at rest, the Lighthill tensor in the right hand-side must contains properly both the sound generation and all flow - acoustics interactions. This implies that the data used to build up the source term must come from compressible simulations where the sound field is correctly calculated. Neverthelesss, most of practical applications use conventional simulation codes. It is therefore generally more convenient to apply Lighthill's theory to predict the noise for flows at low Mach numbers, where mean flow effects on propagation are small. For flows at very low Mach numbers, the direct computation of the sound is moreover difficult owing to the very poor efficiency of sound generation, and Lighthill's equation can easily be solved. For flows at higher Mach numbers, it seems however more natural to use hybrid methods with wave operators including mean flow effects, for example the linearized Euler equations.

## Appendix A: Integral solution of Lighthill's equation in two dimensions

To obtain a time-domain solution of equation (1) for a two-dimensional geometry, we consider the 2-D free-space Green function[23] $G(\mathbf{x},\mathbf{y},t-\tau)$, verifying the wave equation

$$\left(\frac{\partial^2}{\partial t^2} - c_0^2\nabla^2\right) G = \delta(\mathbf{x}-\mathbf{y})\,\delta(t-\tau)$$

and written as

$$G(\mathbf{x},\mathbf{y},t-\tau) = \frac{H(t-\tau-r/c_0)}{2\pi c_0^2\sqrt{(t-\tau)^2 - r^2/c_0^2}}$$

where $r = |\mathbf{x}-\mathbf{y}|$ is the distance from the source to the observer. A solution of equation (1) is given by the convolution of the Green function with the source term $S_{ij} = \partial^2 T_{ij}/\partial y_i \partial y_j$ of Lighthill's equation. Therefore, the solution is

$$\rho'(\mathbf{x},t) = \iint_{-\infty}^{+\infty} G(\mathbf{x},\mathbf{y},t-\tau) S_{ij}(\mathbf{y},\tau)\,d\tau d\mathbf{y}$$

and can be written, owing to the properties of the Heaviside function, as

$$\rho'(\mathbf{x},t) = \frac{1}{2\pi c_0^2}\int_{S_y}\int_{-\infty}^{t-r/c_0} \frac{S_{ij}(\mathbf{y},\tau)}{\sqrt{(t-\tau)^2 - r^2/c_0^2}} d\tau d\mathbf{y}$$

where $S_y$ is the source region. Evaluating this expression is difficult because the lower limit of the time integral is infinite, and a truncation of the time integration in numerical simulation can lead to inaccuracies.

To avoid theses difficulties, two-dimensional problems are commonly solved into the frequency domain[24,25] where the wave equation is expressed in the form of a Helmholtz equation. By applying the Fourier transform $\mathcal{F}$ such as $\widehat{\phi}(\mathbf{x},\omega) = \mathcal{F}[\phi(\mathbf{x},t)]$, equation (1) becomes

$$\left(\omega^2 + c_0^2\nabla^2\right)\widehat{\rho}(\mathbf{x},\omega) = -\widehat{S_{ij}}(\mathbf{x},\omega) \tag{5}$$

The two-dimensional Green function associated to this equation is

$$\widehat{G}(\mathbf{x},\mathbf{y},\omega) = \frac{i}{4c_0^2} H_0^{(2)}\left(\frac{\omega r}{c_0}\right)$$

where $H_0^{(2)}$ is the Hankel function of the second kind and order zero. A solution of equation (5) is found by convolution with the Green function and is given by

$$\widehat{\rho'}(\mathbf{x},\omega) = -\int_{S_y} \widehat{G}(\mathbf{x},\mathbf{y},\omega)\widehat{S_{ij}}(\mathbf{y},\omega)\,d\mathbf{y}$$

For an unbounded fluid, the differential operator in $\widehat{S_{ij}}$ can be applied to either $\widehat{G}$ or $\widehat{T_{ij}}$. Thus

$$\widehat{\rho'}(\mathbf{x},\omega) = -\int_{S_y} \widehat{T_{ij}}(\mathbf{y},\omega)\frac{\partial^2 \widehat{G}}{\partial y_i \partial y_j}(\mathbf{x},\mathbf{y},\omega) d\mathbf{y} \tag{6}$$

This is the solution of Lighthill's equation practically used in this work for two-dimensional problems.

## Acknowledgments

The authors gratefully acknowledge Xavier Gloerfelt for providing the frequency-domain solver of Lighthill's equation and for stimulating discussions. Computing time is supplied by Institut du Développement et des Ressources en Informatique Scientifique (IDRIS - CNRS).

## References

[1]Lighthill, M.J., 1952, On sound generated aerodynamically - I. General theory, *Proc. Roy. Soc. London*, **211**, Ser. A, 1107, 564-587.

[2]Ribner, H.S., 1969, Quadrupole correlations governing the pattern of jet noise, *J. Fluid Mech.*, **38**(1), 1-24.

c)2001 American Institute of Aeronautics & Astronautics or Published with Permission of Author(s) and/or Author(s)' Sponsoring Organization.

[3]BAILLY, C., LAFON, P. & CANDEL, S., 1997, Subsonic and supersonic jet noise prediction from statistical source models, *AIAA Journal*, **35**(11), 1688-1696.

[4]BASTIN, F., LAFON, P. & CANDEL, S., 1997, Computation of jet mixing noise due to coherent structures: the plane jet case, *J. Fluid Mech.*, **335**, 261-304.

[5]SHIH, S.H., HIXON, D.R., MANKBADI, R.R., PILON, A. & LYRINTZIS, A., 1997, Evaluation of far-field jet noise prediction methods, AIAA Paper 97-0282.

[6]BOGEY, C., BAILLY, C. & JUVÉ, D., 2000, Numerical simulation of the sound generated by vortex pairing in a mixing layer, *AIAA Journal*, **38**(12), 2210-2218.

[7]SEROR, C., SAGAUT, P., BAILLY, C. & JUVÉ, C., 2000, Sound generated by high speed rectangular jet using Large Eddy Simulation, 7$^{\text{th}}$ International Congress on Sound and Vibration, Garmish-Partenkirchen.

[8]MITCHELL, B.E., LELE, S.K. & MOIN, P., 1999, Direct computation of the sound generated by vortex pairing in an axisymmetric jet, *J. Fluid Mech.*, **383**, 113-142.

[9]COLONIUS, T. & FREUND, J.B., 2000, Application of Lighthill's equation to a Mach 1.92 turbulent jet, *AIAA Journal*, **38**(2), 368-370.

[10]PHILLIPS, O.M., 1960, On the generation of sound by supersonic turbulent shear layers, *J. Fluid Mech.*, **9**(1), 1-28.

[11]LILLEY, G.M., 1972, The generation and radiation of supersonic jet noise. Vol. IV - Theory of turbulence generated jet noise, noise radiation from upstream sources, and combustion noise. Part II: Generation of sound in a mixing region, *Air Force Aero Propulsion Laboratory*, AFAPL-TR-72-53, Vol. 4.

[12]COLONIUS, T., LELE, S.K. & MOIN, P., 1997, Sound generation in a mixing layer, *J. Fluid Mech.*, **330**, 375-409.

[13]BAILLY, C., BOGEY, C. & JUVÉ, D., 2000, Computation of flow noise using source terms in linearized Euler's equations, AIAA Paper 2000-2047.

[14]RIBNER, H.S., 1977, On the role of the shear term in jet noise, *J. Sound Vib.*, **52**(1), 121-132.

[15]RAHIER, G & REDONNET, S., 2000, Application de l'équation de Lighthill au calcul de rayonnement acoustique en présence d'un écoulement non uniforme, Report of ONERA, No. RT 3/8020 DSNA/N.

[16]MICHALKE, A., 1964, On the inviscid instability of the hyperbolic-tangent velocity profile, *J. Fluid Mech.*, **19**, 543-556.

[17]BOGEY, C., BAILLY, C. & JUVÉ, D., 2000, Computation of the sound radiated by a 3-D jet using Large Eddy Simulation, AIAA Paper 2000-2009.

[18]BOGEY, C., 2000, Calcul direct du bruit aérodynamique et validation de modèles acoustiques hybrides, Ph. D. Thesis of Ecole Centrale de Lyon, No. 2000-11.

[19]INOUE, O, HATTORI, Y & SASAKI, T., 2000, Sound generation by coaxial collision of two vortex rings, *J. Fluid Mech.*, **424**, 327-365.

[20]MÖHRING, W., 1978, On vortex sound theory at low Reynolds number, *J. Fluid Mech.*, **85**, 685-691.

[21]BRIDGES, J. & HUSSAIN, F., 1992, Direct evaluation of aeroacoustic theory in a jet, *J. Fluid Mech.*, **240**, 469-501.

[22]BASTIN, F., 1995, Étude numérique du bruit de jet rayonné par les structures cohérentes de la turbulence, Ph. D. Thesis of Ecole Centrale de Paris.

[23]DOWLING, A.P. & FFOWCS WILLIAMS, J.E., 1983, Sound and sources of sound, *Ellis Horwood Limited*, see 2.4: Two-Dimensional Sound Waves, 54-61.

[24]LOCKARD, D.P., 2000, An efficient, two-dimensional implementation of the Ffowcs Williams and Hawkings equation, *J. Sound Vib.*, **229**(4), 897-911.

[25]GLOERFELT, X, BAILLY, C. & JUVÉ, D., 2001, Computation of the noise radiated by a subsonic cavity using direct simulation and acoustic analogy, AIAA Paper 2001-2226.